

# Spin gap formation in the quantum spin systems TiOX, X=Cl and Br

P. Lemmens<sup>1</sup>, K.Y. Choi<sup>2</sup>, R. Valentí<sup>3</sup>, T.

Saha-Dasgupta<sup>4</sup>, E. Abel<sup>5</sup>, Y.S. Lee<sup>5</sup>, and F.C. Chou<sup>6</sup>

<sup>1</sup> *Max Planck Inst. for Solid State Research,*

*D-70569 Stuttgart, and Inst. for Physics of Condensed Matter,*

*Technical University of Braunschweig, D-38106 Braunschweig, Germany*

<sup>2</sup> *Inst. for Materials Research, Tohoku University, Sendai 980-8577, Japan*

<sup>3</sup> *Inst. für Theoretische Physik, Universität Frankfurt, D-60054 Frankfurt, Germany*

<sup>4</sup> *S.N. Bose National Centre for Basic Sciences,*

*Salt Lake City, Kolkata 700098, India*

<sup>5</sup> *Dept. of Physics, MIT, Cambridge, MA 02139, USA and*

<sup>6</sup> *Center for Materials Science and Engineering,*

*MIT, Cambridge, MA 02139, USA*

(Dated: March 23, 2022)

## Abstract

In the layered quantum spin systems TiOCl and TiOBr the magnetic susceptibility shows a very weak temperature dependence at high temperatures and transition-induced phenomena at low temperatures. There is a clear connection of the observed transition temperatures to the distortion of the octahedra and the layer separation. Band structure calculations point to a relation of the local coordinations and the dimensionality of the magnetic properties. While from magnetic Raman scattering only a small decrease of the magnetic exchange by -5-10 % is derived comparing TiOCl with TiOBr, the temperature dependence of the magnetic susceptibility favors a much bigger change.

PACS numbers: 78.30.-j, 75.10.Jm, 75.30.Et

## I. INTRODUCTION

The compounds  $\text{TiOX}$ , with  $\text{X}=\text{Cl}$  and  $\text{Br}$  are formed by layers of distorted  $\text{TiO}_4\text{X}_2$  octahedra. Quantum magnetism in these systems is based on the  $\text{Ti}^{3+}$  ions with one electron ( $3d^1$ ,  $s=1/2$ ) in a  $t_{2g}$  state. The distortion of the octahedra leads to the predominant occupation of  $d_{xy}$  orbitals that form chain-like direct exchange paths of orbitals along the crystallographic  $b$  axis of the compound. In several experiments, as magnetic susceptibility<sup>1,2</sup>, NMR<sup>3</sup>, ESR<sup>4</sup>, X-ray scattering<sup>5,6</sup>, Raman scattering and optical spectroscopy<sup>7,8</sup>, strong fluctuations and multiple transitions are observed that are attributed to this spin/orbital system with low dimensionality. So far, with the exception of one IR investigation<sup>9</sup>, only the system  $\text{TiOCl}$  has been investigated thoroughly. The isostructural  $\text{TiOBr}$  has not been in the center of interest due to more severe problems in growing single crystalline samples of sufficient quality. The scaling of the IR active phonon frequencies with the involved ionic masses, however, proposes  $\text{TiOBr}$  as a perfect reference system. The compounds differ crystallographically by an increase of the  $c$  axis lattice parameter from 8.03 to 8.53 Å, going from  $\text{X}=\text{Cl}$  to  $\text{Br}$ . This means that in  $\text{TiOBr}$  the coupling between the planes of octahedra is even less important compared to  $\text{TiOCl}$ . Furthermore, the distortion of the octahedra is larger in  $\text{TiOBr}$ .

The compounds  $\text{TiOX}$  belong to a new class of spin-1/2 transition metal oxides based on  $\text{Ti}^{3+}$  ions in weakly interconnected, distorted octahedral coordinations<sup>2,10,11,12</sup>. Very often these systems show phase transitions into singlet ground states that resemble to the spin-Peierls instability<sup>13</sup>. In contrast to, e.g.  $\text{CuGeO}_3$ <sup>14,15</sup> where the spin-Peierls transition leads to a mean-field size of the reduced gap ratio, very large spin gaps exist in some titanates<sup>11,16</sup>. For  $\text{TiOCl}$  even a pseudo gap for  $T > T_c$  has been reported based on NMR and Raman scattering experiments<sup>3,7</sup>. As  $t_{2g}$  states of the  $\text{Ti}^{3+}$  ions ( $3d^1$ ,  $s=1/2$ ) in perfect octahedral surrounding show orbital degeneracy, it is tempting to assign part of these phenomena to orbital degrees of freedom. Spin-orbital coupled systems have been investigated theoretically with respect to their instabilities<sup>17,18,19,20</sup> and as they are candidates for exotic electronic configurations<sup>1,2,20</sup>. These theoretical scenarios did not explicitly consider static or dynamic phonon degrees of freedom. For 2D systems with low symmetry exchange paths it is known that phonons stabilize spin liquids and shift phase lines<sup>21</sup>. Furthermore, orbital configurations strongly couple to the lattice<sup>22</sup>. Therefore, changes of lattice parameters are expected to affect the magnetic properties and related instabilities of such systems considerably.

In this article we present a comparative study of TiOCl and TiOBr using magnetic susceptibility, Raman scattering and band structure calculations to relate structural and electronic properties of these systems and to achieve a better understanding of the observed instabilities. It is shown, that the fluctuation regime in TiOBr is even more extended compared to TiOCl.

## II. STRUCTURAL ASPECTS OF TIOX

The layered crystal structure of TiOX is formed by  $\text{Ti}^{3+}\text{O}^{2-}$  bilayers, that are separated by  $\text{Cl}^-$  bilayers. The basic  $\text{TiCl}_2\text{O}_4$  units are distorted octahedra that share edges. These units form double layers in the  $ab$  plane of an orthorhombic unit cell with FeOCl-type structure<sup>23,24</sup>. In Fig. 1 (a) a sketch of octahedra within two rows of the double layer is shown. In Fig. 1 (b), (c) local Ti-O-X coordinations are given in the  $bc$  and the  $ab$  plane, respectively. Important structural parameters and atomic distances can be found in Table I to highlight common and emphasize differences induced by substituting Cl and Br ions. It is evident that the substitution leads to a considerable increase of the volume of the unit cell. This effect divides up into an enhanced separation of the layers and to a smaller extend to an elongation of the cell in  $b$  axis direction. The octahedra distortion is more pronounced in TiOBr. This is demonstrated in Table I by comparing the shift of the Ti ion out of the basal plane of the octahedra along the  $c$  axis.

## III. SAMPLE PREPARATION AND EXPERIMENTAL

Single crystals of TiOCl and TiOBr have been grown using a chemical vapor transport method.<sup>2</sup> In the following we will describe the preparation of TiOBr as it is less well established. An initial mixture of  $\text{TiO}_2$ , Ti, and  $\text{TiBr}_4$  with a molar ratio of 4:3:9 was sealed in an evacuated quartz tube. The tube was then placed within a two zone furnace, and a constant thermal gradient was maintained (650°C to 550°C over a 25 cm distance). After approximately 5-8 days, single crystals of TiOBr with sizes up to 5 mm<sup>2</sup> can be extracted. The quality of the TiOBr crystals is similar to the TiOCl crystals investigated in Ref.<sup>2</sup>. However, TiOBr is less stable under ambient conditions, as it readily reacts with water in the air.

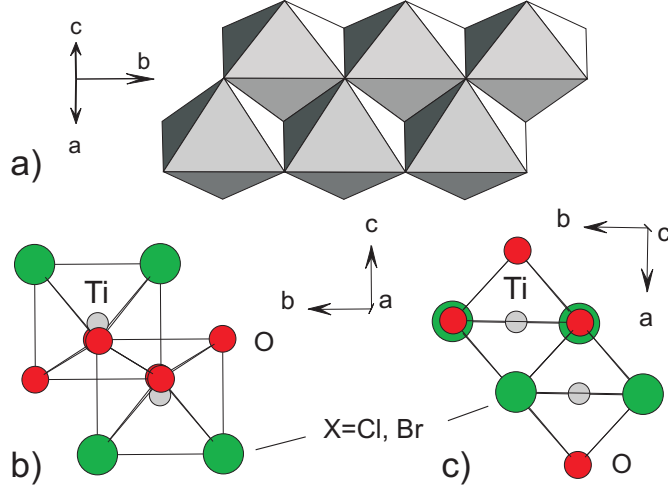


FIG. 1: a) A double layer within the crystallographic  $ab$  plane formed by edge sharing, distorted  $\text{TiCl}_2\text{O}_4$  octahedra. Local coordinations as projected on the a)  $bc$  and c)  $ab$  plane. The relative distances correspond to  $\text{TiOCl}$ .

The magnetic susceptibility has been measured on a single crystal sample of  $\text{TiOBr}$  using a SQUID magnetometer. Raman scattering investigations have been performed using the 514.5 nm excitation wavelength with light polarization parallel to the crystallographic  $b$  axis of the platelet-like ( $ab$  surface) single crystals of  $\text{TiOCl}$  (Ref. 2). No strong resonance effects have been detected comparing 514.5 nm and 488 nm excitation wavelength. A comparison of the phonon spectrum of  $\text{TiOBr}$  with  $\text{TiOCl}$  using optical reflectivity  $R(\omega)$  experiments can be found in Ref. 9. Details related to optical experiments can be found in Ref. 25. A review on the implications of magnetic Raman scattering in low dimensional spin systems is given in Ref. 15.

#### IV. MAGNETIC SUSCEPTIBILITY AND PHASE TRANSITIONS

In Fig. 2 the magnetic susceptibility  $\chi(T)$  of  $\text{TiOBr}$  is given. The open circles are the raw data, and the filled squares are the data after subtraction of a small Curie tail. The general behavior is reminiscent of the susceptibility of  $\text{TiOCl}^{2,3}$  in the sense that above 100 K the magnetic susceptibility  $\chi(T)$  of  $\text{TiOBr}$  is only weakly temperature dependent<sup>1</sup> and forms a broad maximum at  $T_{\text{max}} \sim 210$  K. In contrast to  $\text{TiOCl}$ , the Bonner-Fisher curve does not provide a good fit to the higher temperature behavior of  $\text{TiOBr}$  (not shown here).

TABLE I: Structural parameters and atomic separations for TiOCl and TiOBr with  $Pmmn$  (no. 59). Units are  $\text{\AA}$  or  $\text{\AA}^3$ . Parameters are rounded for clarity and derived using Refs. 23 and 24. Intra-layer Ti-Ti separations are given along the direct exchange path parallel to the  $b$  axis and from the upper to the lower Ti site of one double layer. For the inter-layer Ti-Ti separations also two values exist due to the double layers. The distortions of the octahedra are characterized by  $\Delta c_{Ti}$ , corresponding to the  $c$  axis shift of the Ti ion out of its basal plane.

	lattice parameters	TiOCl	TiOBr	$10^2 \cdot \Delta x/x$
unit cell	a	3.79	3.79	$\pm 0.0$
	b	3.38	3.49	+ 3.3
	c	8.03	8.53	+ 6.2
	volume	102.9	112.6	+ 9.4
intra-double layer	Ti - Ti <sub>b</sub>	3.38	3.49	+ 3.2
	Ti - Ti <sub>bc</sub>	3.2	3.19	- 0.3
inter-double layer	Ti - Ti <sub>c</sub>	6.58	7.12	+ 8.2
	Ti - Ti <sub>c</sub>	8.13	8.91	+ 9.6
distortion	$\Delta c_{Ti}$	$5.5 \cdot 10^{-2}$	$6.1 \cdot 10^{-2}$	+ 10.9

At low temperatures, there is a dramatic drop in the susceptibility at  $T_{c1}^{\text{Br}}=28$  K. X-ray scattering in TiOCl has revealed a commensurate dimerization for  $T < T_{c1}^{\text{Cl}}=67$  K along the  $b$  axis.<sup>5,6</sup> Thereby, the crystal structure changes from  $Pmmn$  to  $P2_1/m$  with atomic displacements restricted to the  $bc$  plane. The flat susceptibility for  $T < T_{c1}$  is therefore taken as an indication for a similar structural distortion in TiOBr that accompanies the spin gap formation. It has been highlighted, that with the exception of the comparably large spin gap the resulting low temperature state of the two systems is very well comparable to other spin-Peierls systems<sup>7,8</sup>.

The inset shows the normalized susceptibility  $(\chi - \chi_0)/\chi_{max}$  of both systems vs.  $T_{c1}$  and vs.  $T_{c2}$  of the respective compound.  $\chi_0$  has been extrapolated in the limit  $T \rightarrow 0$ . From these data it is evident that the overall susceptibilities scale very well with respect to  $T_{c1}$ . This refers mainly to the decrease that is observed towards lower temperatures. Smaller deviations exist in the temperature regime  $T_{c1} < T < 2T_{c1}$  and a close inspection of

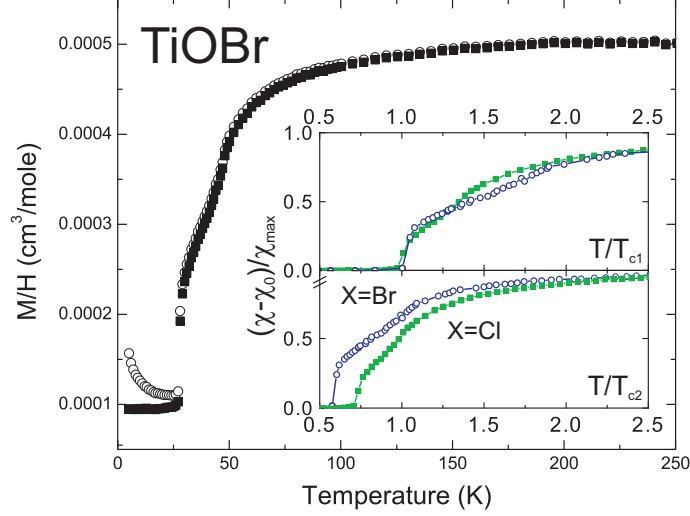


FIG. 2: (color online) Magnetic susceptibility ( $M/H$ ) of TiOBr with a magnetic field of 1 Tesla parallel to the  $ab$  plane. Open (full) symbols corresponds to the as measured data (data after subtracting a defect contribution). The upper and lower inset show the scaled susceptibility  $(\chi - \chi_0)/\chi_{max}$  vs.  $T/T_{c1}$  or vs.  $T/T_{c2}$  for TiOX,  $X=\text{Cl}$  and Br. The transition temperatures are given in Table II.

the susceptibility data reveals a second critical temperature  $T_{c2}^{\text{Br}}=47$  K at which the change of susceptibility is most pronounced. At the corresponding temperature  $T_{c2}^{\text{Cl}}=92$  K of TiOCl evidence for incommensurate distortions has been found together with anomalies in the specific heat<sup>6</sup>. Some results of the magnetic characterization are summarized in Table II.

In the lower inset of Fig. 2 the magnetic susceptibility is plotted with respect to the higher characteristic temperature. The decrease of the magnetic susceptibility does not scale well with  $T_{c2}$ . As this decrease is related to the opening and magnitude of the spin gap  $\Delta(T)$  at the respective temperature,  $T_{c2}$  cannot be directly related to the spin gap formation.

The scaling behavior may be further investigated comparing ratios of the critical temperatures and the maxima of the susceptibility  $\chi(T)$ . The maximum in  $\chi(T)$  gives some information about an averaged magnetic coupling strength. According to Cross and Fisher<sup>26</sup> a linear relation between  $T_c$  and the exchange coupling  $J$  is expected for spin-Peierls systems with  $T_c/J = 0.8\lambda$  and a spin phonon coupling  $\lambda$ . In Table II the corresponding ratios are given. It is noteworthy, that in contrast to the decrease of the susceptibility its maximum position scales with the higher transition temperature. Comparing these characteristic tem-

TABLE II: Magnetic parameters from TiOCl and TiOBr determined from susceptibility, the maxima positions in Raman scattering data, the exchange coupling parameters from downfolding the bandstructure and their change in % with respect to TiOCl.

	TiOCl	TiOBr	$10^2 \cdot \Delta x/x$
$T_{c1}$	67 K	28 K	- 58.2
$T_{c2}$	92 K	47 K	- 48.9
$T_{max}$ in $\chi(T)$	400 K	210 K	- 47.5
$T_{c1}/T_{max}$	0.16	0.13	-
$T_{c2}/T_{max}$	0.23	0.22	-
$\Delta\omega_{max}^1$	928 $\text{cm}^{-1}$	875 $\text{cm}^{-1}$	- 5.7
$\Delta\omega_{max}^2$	1404 $\text{cm}^{-1}$	1390 $\text{cm}^{-1}$	- 1.0
$J_{d-xy}^{\text{downfolding}}$	621 K	406 K	- 35

peratures the following ratios are determined:  $T_{c1}^{\text{Cl}}/T_{c1}^{\text{Br}} = 2.4$ ,  $T_{c2}^{\text{Cl}}/T_{c2}^{\text{Br}} = 1.96$ , while the maximum temperatures give  $T_{\text{max}}^{\text{Cl}}/T_{\text{max}}^{\text{Br}} = 1.91$ . Especially the latter two ratios show a good matching and lead to the conclusion that the characteristic energy scales of the thermodynamic quantities differ roughly by a factor of two between the two systems. This conclusion does not perfectly match to the calculated hopping integral  $t$  given in Table III and results from high energy Raman scattering discussed below.

For TiOCl large fluctuations have been reported at high temperatures ( $T > T_{c1}$ ) based on anomalies in the  $^{47,49}\text{Ti}$  spin relaxation rate and a strong temperature dependence of the ESR-derived  $g$ -factor<sup>3,4</sup>. These observations lead to the assignment of a fluctuation or pseudo gap temperature at  $T^*=135$  K. For the temperature regime  $T_{c1} < T \leq T^*=135$  K also pronounced anomalies and softenings of the Raman-active optical phonon modes exist<sup>7</sup>. Furthermore, the spin gap  $E_g = 430$  K determined from NMR<sup>3</sup> is very large. The reduced gap ratios are  $2E_g/k_B T_{c1,c2} = 10 - 15$ .

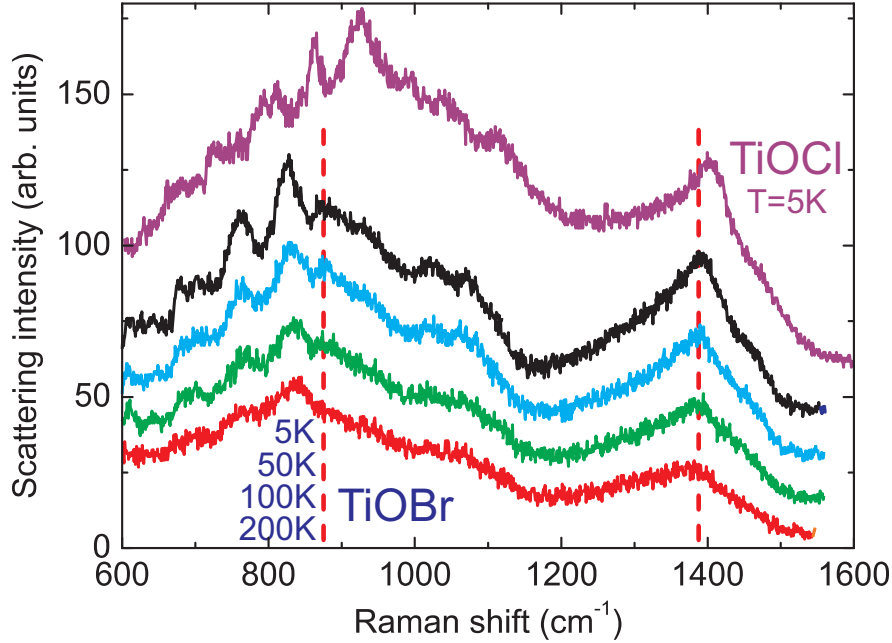


FIG. 3: (color online) High energy Raman scattering for TiOX with X=Cl and Br with light polarization parallel to the crystallographic  $b$  axis,  $c(bb)-c$ . The data are shifted for clarity. The dashed vertical lines denotes the position of the maxima observed in TiOCl.

## V. HIGH ENERGY RAMAN SCATTERING

In Fig. 3 the Raman scattering intensity of TiOCl ( $T=5$  K) and TiOBr ( $5 \text{ K} < T < 200 \text{ K}$ ) is given in the frequency regime that is characteristic for magnetic scattering. Typical energies of two magnetic exchange scattering are estimated within an Ising-like picture counting the number of broken bonds that an exchange process leaves behind. Using the coupling constant  $J=660 \text{ K}$  for TiOCl from magnetic susceptibility<sup>2</sup>, magnetic light scattering should have typical energies between  $2 \cdot J=920 \text{ cm}^{-1}$  and  $4 \cdot J=1800 \text{ cm}^{-1}$ . The exchange pathes considered theoretically have both one dimensional and two dimensional aspects<sup>22</sup>. For TiOCl two broad maxima are observed, a symmetric one at  $928 \text{ cm}^{-1}$  ( $2 \cdot J=917 \text{ cm}^{-1}$ ) and an asymmetric one at  $1404 \text{ cm}^{-1}$  ( $3 \cdot J=1375 \text{ cm}^{-1}$ ). For TiOBr the overall spectral distribution of scattering intensity has a similar shape. The maxima are at  $\Delta\omega_{\text{max}}^{\text{Br}-1}=875 \text{ cm}^{-1}$  and  $\Delta\omega_{\text{max}}^{\text{Br}-2}=1390 \text{ cm}^{-1}$ , i.e. they are shifted by 5% and 1%, respectively, to lower frequencies. At low and intermediate energies, pronounced oscillations or superstructures are observed with peak frequencies  $\Delta\omega_{\text{max}}^{\text{Br}-i}=695, 763, 825$  and  $883 \text{ cm}^{-1}$ . These structures have a mean

separation of  $63 \text{ cm}^{-1}$  and are even more pronounced compared to TiOCl.

The double peak structure with additional modulations at low and intermediate energies is a complex structure compared to the observations in other 1D or 2D quantum spin systems. The line shape of such scattering intensity is usually a result of strong magnon-magnon interactions and the local exchange topology. Magnon-magnon interaction leads to a characteristic renormalization and broadening of the spectral weight to lower energy<sup>27</sup>. In undoped high temperature superconductors with  $\text{CuO}_2$  planes that represent a 2D  $s=1/2$  Heisenberg magnet, a single, broadened peak with a maximum at  $\Delta\omega_{\text{max}}^{\text{HTSC}} \approx 2.8 \cdot J$  is observed<sup>28,29,30</sup>. Also in  $\text{Cu}_2\text{Te}_2\text{O}_5\text{Br}_2$ , based on weakly coupled spin tetrahedra, a single symmetric maximum has been observed at  $\Delta\omega_{\text{max}} \approx 2 \cdot J$ <sup>31,32,33</sup>. Well-defined double peak structures have, however, been observed in the 2D nickelates  $\text{La}_{2-x}\text{Sr}_x\text{NiO}_{4+d}$  if stripe domains with a modulation of spin/charge exist. The two maxima are then the result of exchange processes across and within the antiferromagnetic domain walls and they are related to the exchange coupling as  $3 \cdot J$  and  $4 \cdot J$  for a Sr doping of  $x=1/3$ <sup>34,35,36</sup>. For TiOCl recently evidence for a more complex structure of dimerized Ti sites has been obtained from structural investigations<sup>6</sup>. It is proposed, that antiphase domain walls exist within the  $ab$  planes that separate nano domains of different dimer orientations. This situation resembles to some extent the situation in the 2D nickelates and may be the reason for the two maxima.

In the respective frequency range also excitation of other origin can contribute. Here multi-phonon scattering<sup>37</sup> or magnon-phonon coupled modes<sup>38</sup> should be discussed. Multi-phonon scattering is frequently observed in isolating transition metal oxides and leads to peak structures with frequencies very close to multiples of the optical phonon frequencies. For the case of TiOCl the Raman allowed phonon modes of the high temperature phase consist of in-phase Cl-Ti ( $203 \text{ cm}^{-1}$ ) and out-of-phase O-Ti ( $365 \text{ cm}^{-1}$ ) and Ti-Cl ( $430 \text{ cm}^{-1}$ ) modes, respectively. The numbers in brackets give the respective frequencies for TiOCl. These Raman-active modes and also the IR-active phonon modes considerable soften with the exchange of Cl by Br following simple scaling relationships<sup>9</sup>. For TiOBr phonon Raman modes are observed at  $144 \text{ cm}^{-1}$ ,  $323 \text{ cm}^{-1}$  and  $413 \text{ cm}^{-1}$ <sup>139</sup>, which correspond to a decrease of the phonon frequencies by 4-29%. It is also expected that the phonon dispersion is less pronounced in TiOBr due to the weaker interplane coupling.

In the high energy regime comparing TiOCl with TiOBr no considerable shift is observed, therefore a dominant contribution of multiphonon scattering to the two maxima is not

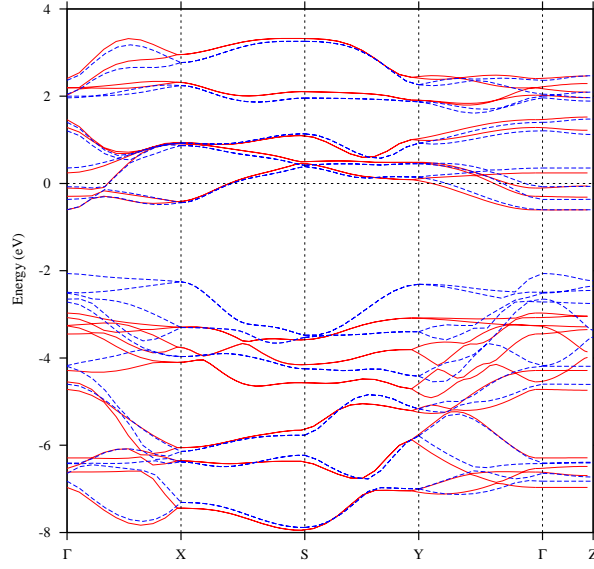


FIG. 4: LDA-bandstructure of TiOCl (solid red line) and TiOBr (dashed blue line) along the path  $\Gamma = (0, 0, 0)$ ,  $X = (0, 1/2, 0)$ ,  $S = (-1/2, 1/2, 0)$ ,  $Y = (-1/2, 0, 0)$ ,  $\Gamma$ ,  $Z = (0, 0, 1/2)$  in units of  $2\pi/a$ ,  $2\pi/b$ ,  $2\pi/c$ .

suggested. Furthermore, corresponding multiples of the phonon frequencies do not exist in the high energy Raman spectral range. This statement should be softened with respect to the modulations seen on the left shoulder of the first more symmetric maximum. It has been shown for TiOCl that this modulation has the same frequency as the difference of two optical phonon frequencies<sup>7</sup>. Finally, we can rule out orbital scattering to observed double peak structures as the large distortion should lead to orbital excitations in the range of 0.1-0.3eV. Concluding the Raman scattering results we state that the corresponding exchange coupling constants do only mildly change with composition.

## VI. AB INITIO CALCULATIONS

In order to investigate the electronic properties of TiOX, we carried out density functional calculations for TiOBr and compared with the results obtained for TiOCl<sup>2,22</sup>. We performed our *ab initio* study in the local density approximation (LDA), the generalized gradient approximation (GGA)<sup>40</sup> and in the so-called LDA+U<sup>41</sup> by using the linearized muffin tin orbital (LMTO) method based on the Stuttgart TBLMTO-47 code<sup>42</sup>. The results

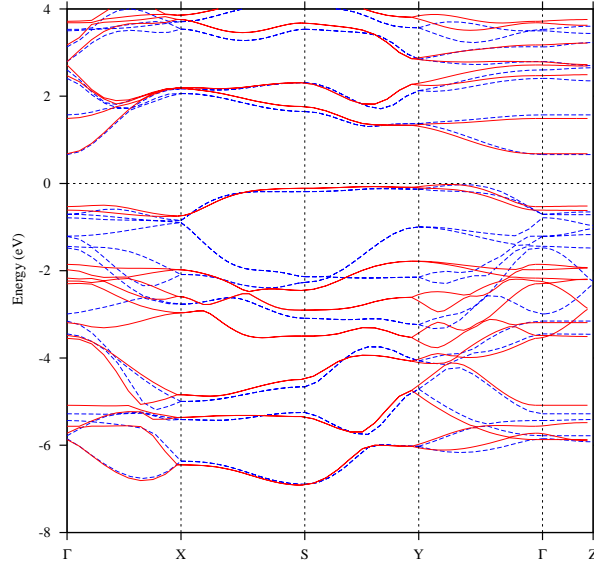


FIG. 5: LDA+U bandstructure of TiOCl (solid red line) and TiOBr (dashed blue line) along the path  $\Gamma$ - X - S - Y -  $\Gamma$  - Z. Note the opening of the gap at the Fermi level with respect to the LDA results. The two bands right below  $E_F$  are of Ti- $d_{xy}$  nature.

within LDA and GGA did not lead to significant differences. An analysis of the TiOBr bandstructure (see Fig. 4) shows that the shape of the LDA- $t_{2g}$  bands crossing the Fermi level have almost identical dispersions to TiOCl<sup>2,22</sup>, what indicates that the exchange paths are similar between these two compounds. Nevertheless, there is in TiOBr a narrowing of the bandwidth along the Y- $\Gamma$ -Z path which is a consequence of the enlargement of the cell in  $b$  and  $c$  directions.

The calculation within the LDA+U approach shows for TiOBr Ti- $d_{xy}$  to be the ground-state as in TiOCl (see Fig. 5 ). In order to get a reliable estimate of the interaction paths in TiOBr, we applied the tight-binding-downfolding procedure<sup>22,43</sup> which obtains the effective Ti- $d_{xy}$ -Ti- $d_{xy}$  hopping parameters by downfolding all the degrees of freedom in the bandstructure calculation other than Ti- $d_{xy}$ . The predominant hopping path in TiOX,  $t$ , is along the nearest neighbor (n.n.) Ti- $d_{xy}$  in the  $b$  direction.  $t = -0.21\text{eV}$  for TiOCl while  $t = -0.17\text{eV}$  for the Br system. This reduction reflects the narrowing of the bands in TiOBr.

A rough estimate of the antiferromagnetic superexchange along  $b$  can be obtained by using the expression  $J = 4t^2/U$  which for  $U=3.3\text{eV}$  is  $J \approx 621\text{ K}$  for TiOCl and  $J \approx 406\text{ K}$

TABLE III: Predominant hopping integrals (in eV)  $t_{i,j}$  for TiOCl and TiOBr obtained from down-folding the bandstructure results (see text). In the Table only the significant digits have been given.

Ti-Ti hopping integrals		TiOCl	TiOBr	$10^2 \cdot \Delta x/x$
$t$	n.n. hopping along $b$	-0.21	-0.17	- 19
$t'_b$	n.n.n. hopping along $b$	-0.03	-0.04	+ 33
$t'$	n.n. hopping along $a$ , same layer	0.04	0.06	+ 50
$t''$	n.n. hopping along $a$ , different layers	0.03	0.04	+ 33

for TiOBr. This change is larger than the shift seen in high energy Raman spectra and in qualitative agreement with the susceptibility measurements. Since we are here interested in estimating the differences between TiOCl and TiOBr, we present in Table III a detailed account of all relevant effective hopping parameters between Ti- $d_{xy}$ -Ti- $d_{xy}$ . We observe that the hopping integrals along other paths than  $t$  are almost an order of magnitude smaller than the main hopping along  $b$ , nevertheless the TiOBr compound has slightly larger effective hoppings along the  $ab$  plane than TiOCl what indicates that in that system the interactions within the  $ab$  plane may be more significant than in TiOCl. The comparison (Table II) shows that this result is only in qualitative agreement with the trend seen in maximum of the magnetic susceptibility.

## VII. SUMMARY AND CONCLUSIONS

The system TiOX, with X=Cl and Br, shows a rich spectrum of anomalies related to electronic, spin and structural degrees of freedom that goes far beyond the scenario of usual spin-Peierls materials<sup>26</sup>. The analysis of the magnetic susceptibility and phase diagram shows that the low temperature transition,  $T_{c1}$ , connected with a commensurate structural distortion, scales with the decrease of the susceptibility and the evolution of the spin gap. The high temperature transition,  $T_{c2}$ , scales with the maximum in the susceptibility that is itself related to the characteristic energy scale of the magnetic system.

The deviations between the latter energy scale and the high energy Raman scattering

are either due to a complex structure of the dimer formation or due to an interplay with the phonon sector. Due to the strong distortion and the already weak interlayer coupling in TiOCl we do not expect that changes of the dimensionality play an essential role.

Finally, our band structure calculations have shown that, although the effective Ti- $d_{xy}$ -Ti- $d_{xy}$  hopping parameters are renormalized with the substitution of Cl by Br, the electronic spectrum does not change drastically. This is in accordance with the high energy Raman scattering. Following the Cross-Fisher scaling, the difference in the transition temperatures of the two compounds should then be attributed both to the smaller electronic bandwidth and a modified spin-phonon coupling. This scenario, however, does neither explain the strong fluctuations nor the large spin gap observed even above the transition temperatures. Further studies on both systems are needed to elucidate these points.

### Acknowledgement

The authors acknowledge fruitful discussions with C. Gros, H. Rosner, L. Degiorgi, E. Ya. Sherman, R. Kremer and B. Keimer. This work was supported by the MRSEC Program of the National Science Foundation under award number DMR 02-13282, and DFG SPP1073.

- 
- <sup>1</sup> R. J. Beynon and J. A. Wilson, J. Phys. Cond. Mat. **5**, 1983 (1993).
  - <sup>2</sup> A. Seidel, C. A. Marianetti, F. C. Chou, G. Ceder, and P. A. Lee, Phys. Rev. **B 67**, 020405 (2003).
  - <sup>3</sup> T. Imai and F. C. Chou, cond-mat/0301425 (2003).
  - <sup>4</sup> V. Kataev, J. Baier, A. Möller, L. Jongen, G. Meyer, and A. Freimuth, Phys. Rev. **B 68**, 140405 (2003).
  - <sup>5</sup> M. Shaz, S. Smaalen, L. Palatinus, M. Hoinkis, M. Klemm, S. Horn, and R. Claessen, cond-mat/040702 (2004).
  - <sup>6</sup> E. Abel, Y. S. Lee, and F. C. Chou, pers. communication (2004).
  - <sup>7</sup> P. Lemmens, K.-Y. Choi, G. Caimi, L. Degiorgi, N. N. Kovaleva, A. Seidel, and F. C. Chou, Phys. Rev. **B 70**, 134429 (2004).
  - <sup>8</sup> G. Caimi, L. Degiorgi, N. N. Kovaleva, P. Lemmens, and F. Chou, Phys. Rev. **B 69**, 125108 (2004).
  - <sup>9</sup> G. Caimi, L. Degiorgi, P. Lemmens, and F. Chou, Journ. Phys.: Cond. Mat. **16**, 5583 (2004).

- <sup>10</sup> E. A. Axtell, T. Ozawa, S. M. Kauzlarich, and R. R. P. Singh, *Journ. Solid State Chem.* **134**, 423 (1997).
- <sup>11</sup> M. Isobe, E. Ninomiya, A. V. Vasil'ev, and Y. Ueda, *Jour. Phys. Soc. Jpn.* **71**, 1423 (2002).
- <sup>12</sup> M. Isobe and Y. Ueda, *J. Phys. Soc. Jpn.* **71**, 1848 (2002).
- <sup>13</sup> J. W. Bray, L. V. Itterante, I. S. Jacobs, and J. C. Bonner, in *Extended Linear Chain Compounds*, edited by J. S. Miller (Plenum Press, New York, 1983), Chap. 7, pp. 353–415.
- <sup>14</sup> M. Hase, I. Terasaki, and K. Uchinokura, *Phys. Rev. Lett.* **70**, 3651 (1993).
- <sup>15</sup> P. Lemmens, G. Güntherodt, and C. Gros, *Physics Reports* **375**, 1 (2003).
- <sup>16</sup> P. Lemmens and P. Millet, in *Quantum Magnetism* (Lecture Notes in Physics, Springer, Heidelberg, 2004), Chap. Spin - Orbit - Topology, a triptych.
- <sup>17</sup> S. K. Pati, R. R. P. Singh, and D. I. Khomskii, *Phys. Rev. Lett.* **81**, 5406 (1998).
- <sup>18</sup> Y. Yamashita, N. Shibata, and K. Ueda, *J. Phys. Soc. Jpn.* **69**, 242 (2000).
- <sup>19</sup> A. K. Koleshuk, H.-J. Mikeska, and U. Schollwöck, *Phys. Rev. B* **63**, 064418 (2001).
- <sup>20</sup> T. Hikiyara and Y. Motome, *cond-mat/0404730* (2004).
- <sup>21</sup> O. A. Starykh, M. E. Zhitomirsky, D. I. Khomskii, R. R. P. Singh, and K. Ueda, *Phys. Rev. Lett.* **77**, 2558 (1996).
- <sup>22</sup> T. Saha-Dasgupta, R. Valentí, H. Rosner, and C. Gros, *Europhys. Lett.* **67**, 63 (2004).
- <sup>23</sup> H. Schaefer, F. Wartenpfehl, and E. Weise, *Zeit. Allg. Anorg. Chem.* **295**, 268 (1958).
- <sup>24</sup> H. Schaefer, H. G. von Schneering, J. Tillock, F. Kuhnen, H. Wohrle, and H. Baumann, *Z. Anorg. Chem.* **353**, 281 (1967).
- <sup>25</sup> G. Caimi, L. Degiorgi, N. N. Kovaleva, P. Lemmens, and F. C. Chou, *Phys. Rev.* **69**, 125108 (2004).
- <sup>26</sup> M. C. Cross and D. S. Fisher, *Phys. Rev. B* **19**, 402 (1979).
- <sup>27</sup> W. Brenig and K. W. Becker, *Phys. Rev. B* **64**, 214413 (2001).
- <sup>28</sup> K. B. Lyons, P. A. Fleury, L. F. Schneemeyer, and J. V. Waszczak, *Phys. Rev. Lett.* **60**, 732 (1988).
- <sup>29</sup> S. Sugai, S. Shamoto, and M. Sato, *Phys. Rev. B* **38**, 6436 (1988).
- <sup>30</sup> S. Sugai, in *Magneto-Optics*, edited by S. Sugano and N. Kojima (Springer, New York, 2000), Vol. 128, Chap. 3. Raman spectroscopy of Magnetic Compounds with Strong Electron-Correlation, pp. 75–106.
- <sup>31</sup> P. Lemmens, K.-Y. Choi, E. E. Kaul, C. Geibel, K. Becker, W. Brenig, R. Valentí, C. Gros, M.

- Johnsson, P. Millet, and F. Mila, Phys. Rev. Lett. **87**, 227201 (2001).
- <sup>32</sup> C. Gros, P. Lemmens, M. Vojta, R. Valentí, K. Y. Choi, H. Kageyama, Z. Hiroi, N. Mushnikov, T. Goto, M. Johnsson, and P. Millet, Phys. Rev. **B 67**, 174405 (2003).
- <sup>33</sup> J. Jensen, P. Lemmens, and C. Gros, Europhys. Lett. **64**, 689 (2003).
- <sup>34</sup> K. Yamamoto, T. Katsufuji, T. Tanaba, and Y. Tokura, Phys. Rev. Lett. **80**, 1493 (1998).
- <sup>35</sup> G. Blumberg, M. V. Klein, and S.-W. Cheong, Phys. Rev. Lett. **80**, 564 (1998).
- <sup>36</sup> V. P. Gnezdilov, A. V. Yermenko, Y. G. Pashkevich, G. G. P. Lemmens, J. M. Tranquada, D. J. Buttrey, and K. Nakajima, Ukr. Journ. Low. Temp. Phys. **28**, 510 (2002).
- <sup>37</sup> K.-Y. C. A. Oosawa, H. Tanaka, and P. Lemmens, subm. to Phys. Rev. B (2004).
- <sup>38</sup> M. Windt, M. Grüninger, T. Nunner, C. Knetter, K. Schmidt, G. Uhrig, T. Kopp, A. Freimuth, U. Ammerahl, B. Büchner, and A. Revcolevschi, Phys. Rev. Lett. **87**, 127002 (2001).
- <sup>39</sup> K. Y. Choi, P. Lemmens, R. Valentí, T. Saha-Dasgupta, and F. C. Chou, in preparation (2005).
- <sup>40</sup> J. P. Perdew, K. Burke, and M. Ernzerhof, Phys. Rev. Lett. **77**, 3865 (1996).
- <sup>41</sup> V. Anisimov, F. Aryasetiawan, and A. I. Lichtenstein, J. Phys.: Condens. Matter **9**, 767 (1997).
- <sup>42</sup> O. K. Andersen, Phys. Rev. Lett. **12**, 3060 (1975).
- <sup>43</sup> O. K. Andersen and T. Saha-Dasgupta, Phys. Rev. **B 62**, R16219 (2000) and references therein.